Field dependence of the carrier occupation in double-quantum-well superlattices

P. Kleinert,* L. Schrottke, and H. T. Grahn
Paul-Drude-Institut für Festkörperelektronik, Hausvogteiplatz 5-7, D-10117 Berlin, Germany

V. V. Bryksin
Physical Technical Institute, Politekhnicheskaya 26, 194021 St. Petersburg, Russia
(Received 8 May 2002; published 6 May 2003)

The field-dependent carrier redistribution is calculated for double-quantum-well superlattices. Kinetic equations for the canonically transformed density matrix are solved analytically. At prevented crossings, when the levels of different quantum wells are aligned by the electric field, an appreciable field-induced carrier redistribution is predicted to occur. With increasing electric field, the subband populations change gradually and the levels exchange their role with respect to the ground state. This predicted carrier redistribution is compared with experimental results.

DOI: 10.1103/PhysRevB.67.195306 PACS number(s): 73.50.Fq, 72.20.Ht

I. INTRODUCTION

Many years after Kazarinov and Suris had published their pioneering theoretical investigations on intersubband effects in semiconductor superlattices (SL's),[1–3] quantum-cascade lasers (QCL's) were realized,[4] which marked a milestone in the history of semiconductor devices. These unipolar semiconductor laser structures, which generate coherent light in the infrared spectral region by exploiting nonequilibrium carrier dynamics, have been the subject of an extraordinary research activity both in basic and applied physics.

Many theoretical approaches have been used to study tunneling and intersubband transitions in SL's, quantum well systems, and QCL's. Based on kinetic equations for the density matrix, the relaxation kinetics of QCL's has been studied by emphasizing the important role of nonequilibrium phonons at the threshold current.[5,6] Other theoretical approaches relied on coupled rate equations,[7,8] calculated characteristic carrier relaxation times,[9–11] or focused on important peculiarities such as the energy-band nonparabolicity.[12] Recently, a kinetic treatment based on the Monte Carlo method has been reported,[13–15] which allows the consideration of a large variety of scattering mechanisms in a realistic manner. Among the most important issues with respect to the design of inter-subband lasers is the optimization of the gain.[16,17]

The long standing proposal by Kazarinov and Suris[1–3] for the utilization of intersubband transitions to obtain midinfrared lasing action has not been demonstrated in simple SL's, but only in structures composed of a sequence of active regions alternating with electron injectors. The injector has the function of an electron reservoir, which supplies carriers into the active region via resonant tunneling, when an appropriate bias is applied so that the ground state of the injector becomes degenerate with the excited state of the active region. Despite a recent proposal of an injectorless QCL,[18] a laser design based exclusively on a single, relatively simple SL has not been realized to our knowledge. There are theoretical considerations claiming that an intrinsic population inversion could occur in SL's due to Wannier-Stark (WS) localization[8] and resonant tunneling.[19] These theoretical studies refer to comparatively simple SL structures, which contain at least two subbands in each well. The flexibility of the SL design, however, is extremely rich. We may think of SL's with different wells in each cell containing several subbands. The potential of such structures seems to be unlimited. Their theoretical study can elucidate the mechanism of field-induced carrier redistribution and allows the formulation of conditions for achieving a population inversion. These theoretical efforts have to be paralleled by experimental studies.

In this paper, we will focus on the field-mediated carrier redistribution, which appears in simple double-quantum-well SL's. As a field-induced population inversion is not expected to occur in such simple structures, the treated system has no direct relevance for QCL applications. It is rather our intent to clarify basic physical properties of the field-induced carrier transport in SL's by applying an analytical approach and by comparing the theoretical results with experimental data obtained from photoluminescence (PL) spectroscopy. We will focus on a double-quantum-well SL, for which an experimental technique has been developed to determine the subband population.[20] In Sec. II, the scattering-free part of the Hamiltonian is exactly diagonalized. The kinetic equations for the density matrix are derived and discussed in Sec. III. We will exclusively treat scattering between electrons and polar-optical phonons. In Sec. IV, the field-induced carrier redistribution is calculated and qualitatively compared with experimental results obtained from PL measurements. It is shown that the observed formal population inversion is due to anticrossings of the WS ladder. Section V summarizes our results.

II. THE HAMILTONIAN

Let us consider a tight-binding model of a SL with two wells in each cell. The scattering-free part of the Hamiltonian has the form

$$H_0=\sum_{m\nu}\sum_{\mathbf{k}_\perp}\varepsilon_\nu(\mathbf{k}_\perp)a^+_{m\nu}(\mathbf{k}_\perp)a_{m\nu}(\mathbf{k}_\perp)+\sum_{mm'}\sum_{\nu\nu'}\sum_{\mathbf{k}_\perp}J_{\nu\nu'}(m-m')a^+_{m\nu}(\mathbf{k}_\perp)a_{m'\nu'}(\mathbf{k}_\perp)-e\mathbf{E}\cdot\sum_{m\nu}\sum_{\mathbf{k}_\perp}\mathbf{R}_{m\nu}a^+_{m\nu}(\mathbf{k}_\perp)a_{m\nu}(\mathbf{k}_\perp), \quad (1)$$

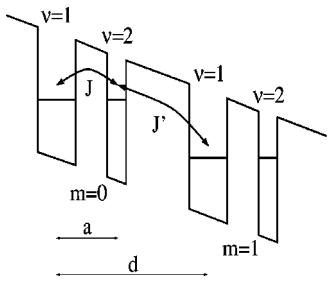

FIG. 1. Schematic diagram of a biased double-quantum-well SL. m indicates the SL cell and $\nu=1,2$ the wells within each cell. The tight-binding parameters J and J' denote the intracell and intercell coupling, respectively. d is the SL period and a the separation of the wells within a given cell.

where $\varepsilon_\nu(\mathbf{k}_\perp)$, $J_{\nu\nu'}$, and $\mathbf{E}$ denote the dispersion relation of the lateral electron motion, the overlap integrals of the tight-binding model, and the electric field vector, respectively. $a^+_{m\nu}(\mathbf{k}_\perp)$ $[a_{m\nu}(\mathbf{k}_\perp)]$ creates [annihilates] an electron in the νth well of the mth SL cell with the lateral momentum $\mathbf{k}_\perp$. The lattice vector $\mathbf{R}_{m\nu}=\mathbf{R}_m+\boldsymbol{\rho}_\nu$ is given by the SL period ($R_{mz}=md$) and the position of each well in a given cell ($\rho_{\nu=1}=0$, $\rho_{\nu=2}=a$). Figure 1 illustrates the energy scheme, when an electric field is applied to the double-quantum-well SL along the growth direction. In our simple tight-binding model, coupling is taken into account only between nearest neighbors. After switching to the full $\mathbf{k}$-space representation via a Fourier transformation

$$a_{m\nu}(\mathbf{k}_\perp)=\sum_{k_z} a_\nu(\mathbf{k})e^{ik_zR_{mz}}, \tag{2}$$

the Hamiltonian is given by

$$\begin{aligned} H_0=&\sum_{\mathbf{k}\nu}\tilde{\varepsilon}_\nu(\mathbf{k}_\perp)a^+_\nu(\mathbf{k})a_\nu(\mathbf{k}) \\ &+\sum_{\mathbf{k}}\left[J_{k_z}a^+_1(\mathbf{k})a_2(\mathbf{k})+J^*_{k_z}a^+_2(\mathbf{k})a_1(\mathbf{k})\right] \\ &+ieE_z\sum_{\mathbf{k}\nu}\frac{\partial}{\partial\kappa_z}a^+_\nu\left(\mathbf{k}_\perp,k_z+\frac{\kappa_z}{2}\right)a_\nu\left(\mathbf{k}_\perp,k_z-\frac{\kappa_z}{2}\right)\Bigg|_{\kappa_z=0}, \end{aligned} \tag{3}$$

where the k_z-dependent effective coupling constant

$$J_{k_z}=J+J'e^{ik_zd} \tag{4}$$

is composed of tight-binding parameters, which couple two wells of adjacent cells (J') and two wells within a single cell (J) (see Fig. 1). E_z denotes the z component of the electric field vector. The dispersion relation of the two subbands is given by $\tilde{\varepsilon}_1(\mathbf{k}_\perp)=\varepsilon(\mathbf{k}_\perp)$ and $\tilde{\varepsilon}_2(\mathbf{k}_\perp)=\varepsilon(\mathbf{k}_\perp)+\varepsilon_g-eE_za$, where ε_g is the energy separation between the two levels at vanishing electric field ($E_z=0$). As it is expected, our approach is independent of the choice, which defines the SL cell. By a simple phase shift of the form $a_2(\mathbf{k})\rightarrow a_2(\mathbf{k})\exp(-ik_zd)$, $a_1(\mathbf{k})\rightarrow a_1(\mathbf{k})$, the two quantum wells are grouped in an alternative manner, which leads to an equivalent model.

In this paper, we do not take into account a possible nonparabolicity in the in-plane band structure and assume equal effective masses in each well $\varepsilon(\mathbf{k}_\perp)=\hbar^2\mathbf{k}^2_\perp/2m$. These assumptions are crucial for our approach and greatly simplify the calculation.

The Hamiltonian H_0 in Eq. (3) is transformed according to

$$a^+_1(\mathbf{k})=\Gamma_1(\mathbf{k})c^+_1(\mathbf{k})-\Gamma^*_2(\mathbf{k})c^+_2(\mathbf{k}), \tag{5}$$

$$a^+_2(\mathbf{k})=\Gamma_2(\mathbf{k})c^+_1(\mathbf{k})+\Gamma^*_1(\mathbf{k})c^+_2(\mathbf{k}), \tag{6}$$

with the normalization condition

$$|\Gamma_1(\mathbf{k})|^2+|\Gamma_2(\mathbf{k})|^2=1. \tag{7}$$

Making use of the canonical transformation (5) and (6), it is easily shown after some elementary algebraic steps that H_0 becomes diagonal, when the function $I(\mathbf{k})=\Gamma_1(\mathbf{k})/\Gamma_2(\mathbf{k})$ satisfies the following Riccati differential equation:

$$[\tilde{\varepsilon}_2(\mathbf{k}_\perp)-\tilde{\varepsilon}_1(\mathbf{k}_\perp)]I(\mathbf{k})+J_{k_z}I(\mathbf{k})^2-J^*_{k_z}-ieE_z\frac{\partial I(\mathbf{k})}{\partial k_z}=0, \tag{8}$$

where periodic boundary conditions are imposed. The linearized version of this equation consists of a set of two linear differential equations[21,22]

$$ieE_z\frac{\partial\Gamma_1(\mathbf{k})}{\partial k_z}=[\xi(\mathbf{k}_\perp)-\varepsilon_-(\mathbf{k}_\perp)]\Gamma_1(\mathbf{k})-J^*_{k_z}\Gamma_2(\mathbf{k}), \tag{9}$$

$$ieE_z\frac{\partial\Gamma_2(\mathbf{k})}{\partial k_z}=[\xi(\mathbf{k}_\perp)+\varepsilon_-(\mathbf{k}_\perp)]\Gamma_2(\mathbf{k})-J_{k_z}\Gamma_1(\mathbf{k}). \tag{10}$$

For the time being, $\xi(\mathbf{k}_\perp)$ is an arbitrary unknown function, which will be determined from the SL periodicity. In Eqs. (9) and (10), we used the abbreviation

$$\varepsilon_-(\mathbf{k}_\perp)=\frac{1}{2}[\tilde{\varepsilon}_1(\mathbf{k}_\perp)-\tilde{\varepsilon}_2(\mathbf{k}_\perp)]. \tag{11}$$

The coefficients of the canonical transformation must satisfy periodic boundary conditions

$$\Gamma_j(\mathbf{k}_\perp,k_z+2\pi/d)=\Gamma_j(\mathbf{k}_\perp,k_z), \tag{12}$$

which we account for by a discrete Fourier transformation

$$\Gamma_j(\mathbf{k}_\perp,k_z)=\sum_{l=-\infty}^{\infty}e^{-ilk_zd}\Gamma_{j,l}(\mathbf{k}_\perp). \tag{13}$$

Applying this transformation to the set of Eqs. (9) and (10), we obtain

$$[\tilde{\xi}(\mathbf{k}_\perp)-\epsilon(\mathbf{k}_\perp)-l]\Gamma_{1,l}(\mathbf{k}_\perp)-A\Gamma_{2,l}(\mathbf{k}_\perp)-B\Gamma_{2,l-1}(\mathbf{k}_\perp)=0, \tag{14}$$

$$[\tilde{\xi}(\mathbf{k}_\perp)+\epsilon(\mathbf{k}_\perp)-l]\Gamma_{2,l}(\mathbf{k}_\perp)-A\Gamma_{1,l}(\mathbf{k}_\perp)-B\Gamma_{1,l+1}(\mathbf{k}_\perp)=0, \tag{15}$$

with $\tilde{\xi}(\mathbf{k}_\perp)=\xi(\mathbf{k}_\perp)/\hbar\Omega$, $A=J/\hbar\Omega$, $B=J'/\hbar\Omega$, and

$$\epsilon(\mathbf{k}_\perp)=\frac{\varepsilon_-(\mathbf{k}_\perp)}{\hbar\Omega}=\frac{a}{2d}-\frac{\varepsilon_g}{2\hbar\Omega}. \tag{16}$$

$\Omega=eE_zd/\hbar$ denotes the Bloch frequency. The last step in the diagonalization procedure of H_0 consists of a discrete Fourier transformation of the field operators

$$c_j(\mathbf{k})=\sum_{l=-\infty}^{\infty}e^{-ilk_zd}c_{j,l}(\mathbf{k}_\perp), \tag{17}$$

which gives us the following final form of the diagonal Hamiltonian:

$$H_0=\sum_{jl}\sum_{\mathbf{k}_\perp}\epsilon_{jl}(\mathbf{k}_\perp)c^+_{j,l}(\mathbf{k}_\perp)c_{j,l}(\mathbf{k}_\perp). \tag{18}$$

Its eigenenergies are

$$\epsilon_{jl}(\mathbf{k}_\perp)=E_j(\mathbf{k}_\perp)-l\hbar\Omega,$$

$$E_j(\mathbf{k}_\perp)=\frac{1}{2}[\tilde{\varepsilon}_1(\mathbf{k}_\perp)+\tilde{\varepsilon}_2(\mathbf{k}_\perp)]\pm\xi(\mathbf{k}_\perp), \tag{19}$$

where the upper sign refers to $j=1$ and the lower one to $j=2$. Within the reduced zone scheme, it is understood that the energy contribution $\xi(\mathbf{k}_\perp)$ to the lateral electron motion is restricted by the requirement $0\leqslant\tilde{\xi}(\mathbf{k}_\perp)=\xi(\mathbf{k}_\perp)/\hbar\Omega\leqslant1/2$. This is an essential condition allowing a determination of $\xi(\mathbf{k}_\perp)$ without any ambiguity. Imposing periodic boundary conditions, Eqs. (9) and (10) are numerically solved relying on the calculational scheme outlined in Ref. 22. The calculation greatly simplifies under the above mentioned parabolicity assumption of the lateral band structure. In this case, the quantities $\Gamma_j(\mathbf{k})$ and $\xi(\mathbf{k}_\perp)$ are independent of $\mathbf{k}_\perp$.

To get an idea of the field-dependent energy spectrum, $\tilde{\xi}$ is calculated as a function of the electric field parameter ϵ. Numerical results are shown in Fig. 2 by the thick solid line. The thin solid lines refer to $-\tilde{\xi}$, $\tilde{\xi}-1$, and $-\tilde{\xi}+1$. If there is no coupling between the layers (A, $B=0$), Eqs. (14) and (15) have the solutions $\tilde{\xi}=\epsilon+l$ and $\tilde{\xi}=-\epsilon+l$ with l being any integer. In this case, the curves in Fig. 2 coalesce to a set of straight lines which cross each other. Coupling leads to anticrossing at field strengths, where tunneling is expected to occur. The main peculiarity is anticipated to appear, when $eE_za=\varepsilon_g$, i.e., when $\epsilon=0$. When the condition $\epsilon=-0.5$ is satisfied, the states of the wells in adjacent cells are at resonance $[eE_z(a+d)=\varepsilon_g]$. Tunneling effects are most pronounced in the vicinity of these anticrossings, the positions of which are renormalized by the coupling parameters J and J'. As already mentioned, the solution $\tilde{\xi}$ we are interested in is confined to the interval $0<\tilde{\xi}<1/2$ (thick solid line in Fig. 2). The anticrossing leads to minigaps with a characteristic field dependence. At $\epsilon=a/2d<1/2$, the electric field goes to infinity ($E_z\to\infty$).

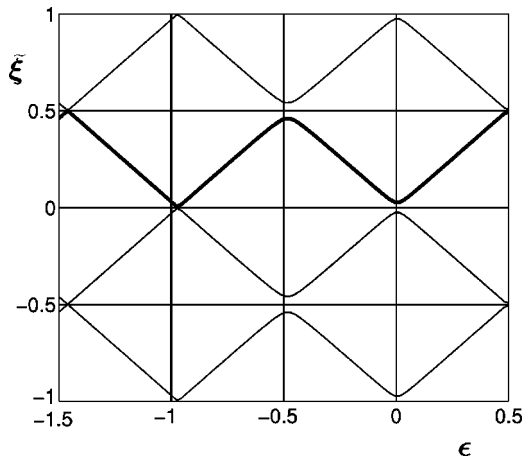

FIG. 2. The energy parameter $\tilde{\xi}=\xi/\hbar\Omega$ as a function of the field parameter $\epsilon=a/(2d)-\varepsilon_g/(2\hbar\Omega)$ (thick solid line) for $J=3$ meV, $J'=1$ meV, $\varepsilon_g=30$ meV, $d=20$ nm, and $a=5$ nm. From bottom to top, the thin solid lines refer to $\tilde{\xi}-1$, $-\tilde{\xi}$ and $-\tilde{\xi}+1$.

Under the condition J and $J'\ll(eE_za-\varepsilon_g)/2$, an analytical solution of Eqs. (9) and (10) can be derived within the WKB approximation by inserting the ansatz

$$\Gamma_j(k_z)=g_j\exp\left[\frac{i}{eE_z}\int_0^{k_z}dk_z'S(k_z')\right], \tag{20}$$

into Eqs. (7), (9), (10), and (12). The WKB solution, valid in the respective branch of the field-dependent energy shift $\xi(\mathbf{k}_\perp)$ is given by

$$\Gamma_1(k_z)=\sqrt{\frac{1}{2}\left(1\pm\frac{\varepsilon_-}{\sqrt{\varepsilon_-^2+|J_{k_z}|^2}}\right)}e^{\pm i[\sigma(k_z)+mk_zd]}$$

$$\text{if}\ \begin{cases}0\leqslant\tilde{\xi}=\lambda-m\leqslant1/2,\\ 0\leqslant\tilde{\xi}=-\lambda+m\leqslant1/2,\end{cases} \tag{21}$$

$$\Gamma_2(k_z)=\sqrt{\frac{1}{2}\left(1\mp\frac{\varepsilon_-}{\sqrt{\varepsilon_-^2+|J_{k_z}|^2}}\right)}e^{\pm i[\sigma(k_z)+mk_zd]}$$

$$\text{if}\ \begin{cases}0\leqslant\tilde{\xi}=\lambda-m\leqslant1/2,\\ 0\leqslant\tilde{\xi}=-\lambda+m\leqslant1/2.\end{cases} \tag{22}$$

m is an appropriate integer chosen in such a way that the inequalities $0\leqslant\tilde{\xi}\leqslant1/2$ are satisfied. The periodic function $\sigma(k_z)$ is calculated from

$$\sigma(k_z)=\frac{1}{eE_z}\int_0^{k_z}dk_z'\left[D(k_z')-\frac{d}{2\pi}\int_0^{2\pi/d}dk_z'D(k_z')\right]$$

$$=\sigma(k_z+2\pi/d) \tag{23}$$

with

$$D(k_z)=\sqrt{\varepsilon_-^2+|J_{k_z}|^2}. \tag{24}$$

The energy shift $\tilde{\xi}$ due to the lateral electron motion is determined from

$$\lambda=\frac{1}{\hbar\Omega}\frac{d}{2\pi}\int_0^{2\pi/d}dk_z D(k_z)$$
$$=\frac{1}{\hbar\Omega}\frac{2}{\pi}\sqrt{\varepsilon_-^2+(J+J')^2}E\left(\sqrt{\frac{4JJ'}{\varepsilon_-^2+(J+J')^2}}\right), \tag{25}$$

where E denotes the complete elliptic integral of the second kind. When the coupling of the wells is very weak, i.e., when they are separated by thick potential barriers ($J,J'\ll\varepsilon_-^2$), the expressions for $\sigma(k_z)$ and λ simplify considerably, and we get

$$\sigma(k_z)=-\frac{\Delta}{2\hbar\Omega}\sin k_z d, \quad \Delta=\frac{2JJ'}{\sqrt{\varepsilon_-^2+(J+J')^2}}, \tag{26}$$

$$\lambda=\frac{1}{\hbar\Omega}\sqrt{\varepsilon_-^2+(J+J')^2}\left[1-\frac{JJ'}{\varepsilon_-^2+(J+J')^2}\right]. \tag{27}$$

Δ corresponds to an effective miniband width, which depends on the electric field and reaches its maximum at the field strength $E_z=\varepsilon_g/(ea)$.

III. THE KINETIC EQUATION

In the previous section, the tight-binding Hamiltonian, which describes carrier motion in double-quantum-well SL's under the influence of a uniform electric field, has been diagonalized exactly. The energy spectrum, obtained from the periodic boundary condition, is characterized by typical anticrossings at tunneling resonances. The exact diagonal form of the one-electron Hamiltonian as given in Eq. (18) can be used as a suitable starting point for many theoretical studies, in which carrier scattering plays an important role. One possibility would be the treatment of small polarons by a second canonical transformation, in which the electron-phonon interaction is involved. Here, we will treat another special case by focusing on weak scattering on polar-optical phonons. For simplicity, we will consider the bulk phonon model. This approach is not chosen to give an accurate representation of real SL systems. Here, it is rather our intent to use a model simple enough for extensive analytical calculations to demonstrate qualitative features in the field-induced carrier redistribution. The lattice constant a_L of the respective bulk material is much smaller than the periodicity d of the SL. Therefore, the phonon wave numbers are restricted to an interval between 0 and $2\pi/a_L$, which is much larger than the first Brillouin zone of the SL ($0\leqslant k_z\leqslant 2\pi/d$). The Hamiltonian of the vibrational subsystem can be written in the form

$$H_{ph}=\sum_{\mathbf{q},\mathbf{G}}\hbar\omega_{\mathbf{q}+\mathbf{G}}b^+_{\mathbf{q}+\mathbf{G}}b_{\mathbf{q}+\mathbf{G}}, \tag{28}$$

where $b^+_{\mathbf{q}+\mathbf{G}}$ and $b_{\mathbf{q}+\mathbf{G}}$ are phonon creation and annihilation operators, respectively. The z components of the reciprocal lattice vector $\mathbf{G}$ are given by $G_z=2\pi m/d$, where $m=0,1,2,\ldots,M$ with $d=Ma_L$. In this representation, the phonon wave vector components q_z are restricted to the first Brillouin zone of the carriers, i.e., $0\leqslant q_z\leqslant 2\pi/d$. The Hamiltonian for the electron-phonon interaction has the form

$$H_{\rm int}=\sum_{\mathbf{k}\nu}\sum_{\mathbf{q},\mathbf{G}}\gamma^\nu_{\mathbf{q}+\mathbf{G}}a^+_\nu(\mathbf{k}+\mathbf{q})a_\nu(\mathbf{k})(b_{\mathbf{q}+\mathbf{G}}+b^+_{-\mathbf{q}-\mathbf{G}}), \tag{29}$$

$$\gamma^\nu_{\mathbf{q}}=\hbar\omega_q\tilde{\gamma}_{\mathbf{q}}e^{iq_z\rho_\nu},$$

where the reciprocal lattice vector $\mathbf{G}$ accounts for Umklapp scattering. Applying the canonical transformation in Eqs. (5) and (6), we obtain

$$H_{\rm int}=\sum_{\mathbf{k},\mathbf{k}'}\sum_{jj'}\sum_{\mathbf{G}}\Lambda^G_{j'j}(\mathbf{k}',\mathbf{k})c^+_{j'}(\mathbf{k}')c_j(\mathbf{k})$$
$$\times[b_{\mathbf{k}'-\mathbf{k}+\mathbf{G}}+b^+_{-\mathbf{k}'+\mathbf{k}-\mathbf{G}}], \tag{30}$$

with coupling terms given by

$$\Lambda^G_{j'j}(\mathbf{k}',\mathbf{k})=\sum_{j_1}\gamma^{j_1}_{\mathbf{k}'-\mathbf{k}+\mathbf{G}}\Gamma^{j_1}_{j'j}(\mathbf{k}',\mathbf{k}). \tag{31}$$

The elements of the Γ matrix can be grouped into the form

$$\Gamma^1_{j'j}(\mathbf{k}',\mathbf{k})=\begin{pmatrix}\Gamma_1(\mathbf{k}')\Gamma_1^*(\mathbf{k}) & -\Gamma_1(\mathbf{k}')\Gamma_2(\mathbf{k})\\ -\Gamma_2^*(\mathbf{k}')\Gamma_1^*(\mathbf{k}) & \Gamma_2^*(\mathbf{k}')\Gamma_2(\mathbf{k})\end{pmatrix}, \tag{32}$$

$$\Gamma^2_{j'j}(\mathbf{k}',\mathbf{k})=\begin{pmatrix}\Gamma_2(\mathbf{k}')\Gamma_2^*(\mathbf{k}) & \Gamma_2(\mathbf{k}')\Gamma_1(\mathbf{k})\\ \Gamma_1^*(\mathbf{k}')\Gamma_2^*(\mathbf{k}) & \Gamma_1^*(\mathbf{k}')\Gamma_1(\mathbf{k})\end{pmatrix}. \tag{33}$$

In the final step, the WS representation (17) is exploited, which leads to the interaction Hamiltonian

$$H_{\rm int}=\sum_{jj'}\sum_{\mathbf{G}}\sum_{\mathbf{k},\mathbf{k}'}\sum_{ll'}\Lambda^G_{j'l',jl}(\mathbf{k}',\mathbf{k})c^+_{j',l'}(\mathbf{k}'_\perp)c_{j,l}(\mathbf{k}_\perp)$$
$$\times[b_{\mathbf{k}'-\mathbf{k}+\mathbf{G}}+b^+_{-\mathbf{k}'+\mathbf{k}-\mathbf{G}}], \tag{34}$$

with the matrix elements

$$\Lambda^G_{j'l',jl}(\mathbf{k}',\mathbf{k})=e^{il'k'_zd}\Lambda^G_{j'j}(\mathbf{k}',\mathbf{k})e^{-ilk_zd}=\Lambda^G_{jl,j'l'}(\mathbf{k},\mathbf{k}')^*. \tag{35}$$

The main quantities, which have to be calculated in order to determine the carrier redistribution, are the elements of the density matrix

$$f^{\alpha'}_{\alpha}(\mathbf{k}_\perp|t)=f^{j'l'}_{jl}(\mathbf{k}_\perp|t)=\langle c^+_{j'l'}(\mathbf{k}_\perp)c_{jl}(\mathbf{k}_\perp)\rangle_t, \tag{36}$$

where α denotes the quantum numbers j and l. The kinetic equation for the density matrix is obtained from the Liouville equation. We will focus on a nondegenerate electron gas, whose equilibrium statistics is given by the Boltzmann distribution function. The structure of the resulting equation

$$\frac{\partial f_{\alpha}^{\alpha'}(\mathbf{k}_\perp|t)}{\partial t}=\frac{i}{\hbar}[\epsilon_{\alpha'}(\mathbf{k}_\perp)-\epsilon_{\alpha}(\mathbf{k}_\perp)]f_{\alpha}^{\alpha'}(\mathbf{k}_\perp|t)$$

$$+\sum_{\beta\beta'}\sum_{\mathbf{k}'_\perp} f_{\beta}^{\beta'}(\mathbf{k}'_\perp|t)W_{\beta,\alpha}^{\beta',\alpha'}(\mathbf{k}'_\perp,\mathbf{k}_\perp) \quad (37)$$

depends mainly on the scattering probability, which relates different subbands and WS ladder states to each other. An explicit expression for the scattering rates $W_{\beta,\alpha}^{\beta',\alpha'}$ is given in Appendix A. The kinetic Eq. (37) for the density matrix allows the simultaneous consideration of coherent and incoherent quantum transport (see, e.g., Ref. 23). From this general result, semiclassical and Boltzmann-like transport equations can be obtained as special cases. To proceed, we remark that due to the periodicity of the SL along the z axis, the density matrix depends only on the difference of WS labels $l-l'$

$$f_{jl}^{j'l'}(\mathbf{k}_\perp|t)=f_{j}^{j'}(\mathbf{k}_\perp,l'-l|t). \quad (38)$$

For high electric fields $\Omega\tau_{\mathrm{eff}}>1$ (τ_{eff} is an effective scattering time), the diagonal elements of the density matrix with respect to a given WS state ($l=l'$) dominate. Here, we consider this case and derive analytical results valid in this high-field regime by keeping only these elements of the distribution function. Furthermore, the off-diagonal elements f_2^1 and f_1^2 of the density matrix give rise to negligible quantum corrections to the stationary carrier redistribution. This has been shown for a QCL structure in Ref. 23. The relevance or irrelevance of the nondiagonal density-matrix elements depends on the representation, in which the kinetic equation is expressed. In our approach, only scattering leads to the off-diagonal terms, which are quickly suppressed by relaxation and dephasing processes. The steady state of our model system is therefore characterized by the kinetic equations

$$\sum_{\mathbf{k}'_\perp} f_1^1(\mathbf{k}'_\perp,0)\sum_{l_1} W_{1l_1,j0}^{1l_1,j0}(\mathbf{k}'_\perp,\mathbf{k}_\perp)$$

$$+\sum_{\mathbf{k}'_\perp} f_2^2(\mathbf{k}'_\perp,0)\sum_{l_1} W_{2l_1,j0}^{2l_1,j0}(\mathbf{k}'_\perp,\mathbf{k}_\perp)=0 \quad (39)$$

valid for $j=1$ and $j=2$. The distribution functions $f_j^j(\mathbf{k}'_\perp,0)$ depend only on $\mathbf{k}_\perp$ via $\varepsilon(\mathbf{k}_\perp)$. This can be used to simplify the $\mathbf{k}_\perp$ integrations. Inserting the scattering probabilities from Eq. (A1) into the Eq. (39), we obtain for $j=1$

$$\sum_{l=-\infty}^{\infty}\{\Phi_{11}(l)(\Theta(\varepsilon+l\hbar\Omega+\hbar\omega_0)[f_1^1(\varepsilon+l\hbar\Omega+\hbar\omega_0)$$
$$-e^{-\beta}f_1^1(\varepsilon)]+\Theta(\varepsilon+l\hbar\Omega-\hbar\omega_0)[e^{-\beta}f_1^1(\varepsilon+l\hbar\Omega$$
$$-\hbar\omega_0)-f_1^1(\varepsilon)])+\Phi_{21}(l)(\Theta(\varepsilon+2\xi+l\hbar\Omega+\hbar\omega_0)$$
$$\times[f_2^2(\varepsilon+2\xi+l\hbar\Omega+\hbar\omega_0)-e^{-\beta}f_1^1(\varepsilon)]+\Theta(\varepsilon+2\xi$$
$$+l\hbar\Omega-\hbar\omega_0)[e^{-\beta}f_2^2(\varepsilon+2\xi+l\hbar\Omega-\hbar\omega_0)-f_1^1(\varepsilon)])\}$$
$$=0 \quad (40)$$

with

$$\Phi_{j'j}(l)=\sum_{q_z}|\Pi_{j'j}(q_z,l)|^2, \quad (41)$$

where $\Pi_{j'j}$ is defined in Eq. (A2). A similar equation is easily derived for $j=2$. If intersubband transitions are neglected ($\Phi_{21}=0$), Eq. (40) reproduces a kinetic equation for the lateral distribution function, which we derived several years ago for SL's with one isolated miniband.[24–26] An exact analytic multiband solution is found in the extreme sequential tunneling limit, when the SL is composed of isolated wells [only $l=0$ in Eq. (40)]

$$f_1^1(\varepsilon)=A\exp\left(-\frac{\varepsilon}{k_BT}\right),\quad f_2^2(\varepsilon)=A\exp\left(-\frac{\varepsilon-2\xi}{k_BT}\right). \quad (42)$$

The constant A is determined from the normalization condition

$$\sum_{\mathbf{k}_\perp}[f_1^1(\mathbf{k}_\perp,0)+f_2^2(\mathbf{k}_\perp,0)]=1. \quad (43)$$

In addition to the special case of isolated double-quantum wells, there is another regime, which is much more interesting and refers to SL's. It admits an analytical solution of the kinetic Eq. (40), too. Usually, in SL's the intrasubband processes are more pronounced than inter-subband transitions. This is the case for weakly coupled SL's, where the term $\Phi_{11}(l=0)\sim 1$ dominates over all other matrix elements $\Phi_{jj'}$ ($j\neq j'$), which are proportional to the tight-binding parameters J and J'. Therefore, a solution of Eq. (40), in which the coupling constant disappeared, can be searched for by a perturbation approach with respect to the small parameters J/ε_g and J'/ε_g. For $l=0$ and $\Phi_{12}=\Phi_{21}=0$, we obtain from the kinetic equations for $j=1$ and $j=2$ the following solution:

$$f_1(\varepsilon)=A_1\exp\left(-\frac{\varepsilon}{k_BT}\right),\quad f_2(\varepsilon)=A_2\exp\left(-\frac{\varepsilon}{k_BT}\right), \quad (44)$$

which is used to derive from Eq. (40) the relation

$$A_1\sum_{l=-\infty}^{\infty}\Phi_{11}(l)(1-e^{l\hbar\Omega/k_BT})$$
$$+\sum_{l=-\infty}^{\infty}\Phi_{21}(l)(A_2-A_1e^{(l\hbar\Omega+2\xi)/k_BT})=0 \quad (45)$$

between the constants A_1 and A_2. Together with the normalization condition in Eq. (43), we have a set of two equations, from which the constants A_1 and A_2 can be calculated.

Again, analytical results can be obtained within the WKB approximation, where the matrix elements $\Phi_{jj'}(l)$ are easily obtained from Eqs. (21), (22), (26), and (41). The result is

$$\Phi_{11}(l)=\Phi_{22}(l)=\frac{1}{2}\left(1+\frac{\varepsilon_-^2}{\varepsilon_-^2+(J+J')^2}\right)F_l\left(\frac{\Delta}{\hbar\Omega}\right), \quad (46)$$

$$\Phi_{12}(l)=\frac{1}{2}\frac{(J+J')^2}{\varepsilon_-^2+(J+J')^2}F_{2m\pm l}\left(\frac{\Delta}{\hbar\Omega}\right)$$

$$\text{if}\ \begin{cases}0\leqslant\tilde{\xi}=\lambda-m\leqslant 1/2,\\ 0\leqslant\tilde{\xi}=-\lambda+m\leqslant 1/2\end{cases} \tag{47}$$

and $\Phi_{21}(l)=\Phi_{12}(-l)$. The effective miniband width Δ enters these equations via the function

$$F_l(x)=\frac{1}{\pi}\int_0^\pi d\varphi J_l^2(x\sin\varphi), \tag{48}$$

where J_l denotes the Bessel function. General expressions for the quantities $\Phi_{jj'}(l)$ and symmetry relations between them can only be obtained numerically from Eqs. (13), (A2), and the definition in Eq. (41). The resulting WS ladder representation

$$\Phi_{11}(l)=\Phi_{22}(l)=\sum_{l'=-\infty}^{\infty}[|\Gamma_{1,l+l'}\Gamma_{1,l'}^*|^2+|\Gamma_{2,l+l'}\Gamma_{2,l'}^*|^2]$$
$$=\Phi_{11}(-l), \tag{49}$$

$$\Phi_{12}(l)=2\sum_{l'=-\infty}^{\infty}|\Gamma_{1,l-l'}\Gamma_{2,l'}|^2=\Phi_{21}(-l) \tag{50}$$

is used to calculate the carrier redistribution in the next sections.

IV. FIELD-INDUCED CARRIER REDISTRIBUTION

A. Theoretical results

Let us calculate the field-induced carrier redistribution from the kinetic equation for the distribution function. The label ν used for the characterization of the multiband SL loses its meaning of a real band index after the canonical transformation (that is the reason why we changed the notation $\nu\rightarrow j$). To calculate the field dependence of the carrier distribution, we have to switch back to the physical picture described by the $\mathbf{k}$-ν representation of the density matrix

$$F_\nu^{\nu'}(\mathbf{k}|t)=\langle a_{\nu'}^+(\mathbf{k})a_\nu(\mathbf{k})\rangle_t. \tag{51}$$

These functions are related to the components of the density matrix $f_j^{j'}(\mathbf{k}_\perp,l-l')$ via the canonical transformation in Eqs. (5) and (6). For the steady state, we obtain the relationship

$$F_1^1(\mathbf{k})-F_2^2(\mathbf{k})=[|\Gamma_1(k_z)|^2-|\Gamma_2(k_z)|^2][f_1^1(\mathbf{k})-f_2^2(\mathbf{k})]$$
$$-4\,\mathrm{Re}\,\Gamma_1(k_z)\Gamma_2(k_z)f_2^1(\mathbf{k}), \tag{52}$$

in which the off-diagonal elements f_2^1 of the density matrix appear. In the Fourier-transformed version of Eq. (52), only the $f_j^{j'}(\mathbf{k}_\perp,l=0)$ components are retained. This is justified in the treated high-field limit. Integrating over $\mathbf{k}_\perp$ and considering Eqs. (44) and (45), we get

$$F_1-F_2=\Delta F_{12}+\sum_{l'=-\infty}^{\infty}(|\Gamma_{1,l'}|^2-|\Gamma_{2,l'}|^2)\frac{\sum_{l=-\infty}^{\infty}\Phi_{21}(l)\left[1-\exp\left(\frac{l\hbar\Omega+2\xi}{k_BT}\right)\right]-\sum_{l=-\infty}^{\infty}\Phi_{11}(l)\left[\exp\left(\frac{l\hbar\Omega}{k_BT}\right)-1\right]}{\sum_{l=-\infty}^{\infty}\Phi_{21}(l)\left[1+\exp\left(\frac{l\hbar\Omega+2\xi}{k_BT}\right)\right]+\sum_{l=-\infty}^{\infty}\Phi_{11}(l)\left[\exp\left(\frac{l\hbar\Omega}{k_BT}\right)-1\right]}, \tag{53}$$

in which the scattering-induced correction $\Delta F_{12}\sim f_2^1$ is negligible in the case of weak electron-phonon coupling. This is seen by solving the kinetic equation in the limit of high electric fields. The contribution to the carrier redistribution, which results from the off-diagonal element f_2^1, is given by

$$\Delta F_{12}=-4\,\mathrm{Re}\sum_{\mathbf{k}_\perp}\sum_{k_z}\Gamma_1(k_z)\Gamma_2(k_z)f_2^1(\mathbf{k}_\perp,0)$$
$$\approx-4\Gamma_{1,0}\Gamma_{2,0}\sum_{j_1l_1}\sum_{\mathbf{k}_\perp\mathbf{k}_\perp'}\frac{f_{j_1}^{j_1}(\mathbf{k}_\perp',0)W_{j_1l_1,20}^{j_1l_1,10}(\mathbf{k}_\perp',\mathbf{k}_\perp)}{\frac{i}{\hbar}[E_2(\mathbf{k}_\perp)-E_1(\mathbf{k}_\perp)]+1/\tau}. \tag{54}$$

The correction ΔF_{12} is estimated by describing the scattering-induced width of the tunneling resonance in Eq. (54) in a phenomenological manner by applying the relaxation-time approximation

$$W_{\alpha,\alpha}^{\alpha',\alpha'}(\mathbf{k}_\perp',\mathbf{k}_\perp)\rightarrow-\frac{1}{\tau}\delta_{\mathbf{k}_\perp',\mathbf{k}_\perp}, \tag{55}$$

to this specific scattering mechanism. While ΔF_{12} is proportional to the small coupling constant of the electron-phonon interaction, all other terms in Eq. (53) are not. A numerical estimate shows that ΔF_{12} can indeed be completely neglected in this equation.

Next let us treat analytical solutions, which are valid for particular cases. When the two wells in each cell are isolated from the neighboring ones, only the $l=0$ terms remain in the l sums, and we obtain from Eqs. (7) and (14), (15)

$$\Gamma_{1,0}=\frac{A}{\tilde{\xi}-\epsilon}\Gamma_{2,0},\quad \Gamma_{1,0}^2+\Gamma_{2,0}^2=1, \tag{56}$$

which together with Eq. (42) leads to

$$F_1 - F_2 = \frac{\epsilon}{\tilde{\xi}} \frac{1-\exp(2\xi/k_BT)}{1+\exp(2\xi/k_BT)} \approx \frac{\varepsilon_g - eE_z a}{2k_BT}, \qquad (57)$$

where $\tilde{\xi} = \sqrt{\epsilon^2 + A^2}$ in the vicinity of $\epsilon = 0$ ($A \ll 1$). The approximation on the right-hand side of Eq. (57) holds in the limit $\xi/k_BT \ll 1$. According to Eq. (57), $F_1 - F_2$ changes its sign at $E_z = \varepsilon_g/ea$ so that a formal population inversion occurs for field strengths larger than $E_z = \varepsilon_g/(ea)$.

Another analytical result can be derived in the WKB approximation. From Eqs. (46), (47) and taking into account

$$\sum_{l=-\infty}^{\infty} F_l\left(\frac{\Delta}{\hbar\Omega}\right) e^{-l\hbar\Omega/k_BT} = I_0^2\left(\frac{\Delta}{\hbar\Omega}\sinh\frac{\hbar\Omega}{2k_BT}\right), \quad \sum_{l=-\infty}^{\infty} F_l\left(\frac{\Delta}{\hbar\Omega}\right) = 1, \qquad (58)$$

we get

$$F_1 - F_2 = \pm \frac{\varepsilon_g - eE_z a}{\sqrt{(\varepsilon_g - eE_z a)^2 + 4(J+J')^2}} \frac{C_\pm - 1}{C_\pm + 1}$$
$$\text{if } \begin{cases} 0 \leqslant \tilde{\xi} = \lambda - m \leqslant 1/2, \\ 0 \leqslant \tilde{\xi} = -\lambda + m \leqslant 1/2 \end{cases} \qquad (59)$$

with

$$C_\pm = e^{\pm 2\lambda \frac{\hbar\Omega}{k_BT}} I_0^2\left(\frac{\Delta}{\hbar\Omega}\sinh\frac{\hbar\Omega}{2k_BT}\right) + \left(1 + \frac{2\varepsilon_-^2}{(J+J')^2}\right) \times \left[I_0^2\left(\frac{\Delta}{\hbar\Omega}\sinh\frac{\hbar\Omega}{2k_BT}\right) - 1\right]. \qquad (60)$$

I_0 is the modified Bessel function. The WKB result in Eq. (59) for the field-induced carrier redistribution simplifies further in the limit of low temperatures ($T \to 0$). In this case, we obtain

$$F_1 - F_2 = \pm \frac{\varepsilon_g - eE_z a}{\sqrt{(\varepsilon_g - eE_z a)^2 + 4(J+J')^2}}$$
$$\text{if } \begin{cases} 0 \leqslant \tilde{\xi} = \lambda - m \leqslant 1/2, \\ 0 \leqslant \tilde{\xi} = -\lambda + m \leqslant 1/2 \end{cases} \qquad (61)$$

which agrees with Eq. (59) in the neighborhood of $eE_z a = \varepsilon_g$ (if $J' = 0$). Again, it is seen that $F_1 - F_2$ changes its sign at $eE_z a = \varepsilon_g$ so that the lower ($\nu = 1$) and upper ($\nu = 2$) subbands exchange their role. The original ground state ($\nu = 1$) becomes the less populated and vice versa. A similar exchange of the role of subbands is predicted by Eq. (61), whenever the electric field satisfies the condition $eE_z(a + nd) = \varepsilon_g$ (with n being a positive integer). This peculiar behavior is confirmed by numerical results for the subband occupation as a function of the electric field, which are derived from Eq. (53) and shown in Fig. 3. The quantities ξ and Γ_{jl} were calculated according to the procedure outlined in Ref. 22. As predicted by the analytical solution in Eq. (61), the two subbands are equally populated, whenever $eE_z(a + nd) = \varepsilon_g$ is fulfilled. At higher electric field strengths, the role played by the two subbands is exchanged. Above the field strength $E_z = \varepsilon_g/(ea)$, the subband $\nu = 1$ is increasingly depopulated with increasing field.

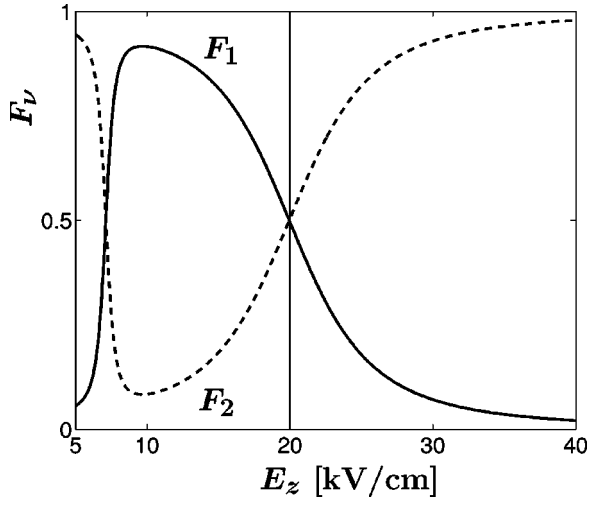

FIG. 3. Field-dependent carrier occupation F_ν of the subband $\nu = 1$ (solid line) and $\nu = 2$ (dashed line) for $J = 3$ meV, $J' = 1$ meV, $\varepsilon_g = 20$ meV, $d = 20$ nm, $a = 5$ nm, and $T = 77$ K.

The monotonous behavior of the occupations F_1 and F_2 at these particular field strengths has to be contrasted with the anti-crossing in the energy diagram shown in Fig. 2. The energy spectrum of the transformed Hamiltonian in Eq. (18) is also characterized by a band index (denoted by j). For a given WS level l, the energy of the constructed subband $j = 1$ is always larger than the energy of the subband $j = 2$. The two subbands are separated by minigaps, in the vicinity of which tunneling becomes important. These peculiarities of the canonically transformed Hamiltonian are masked, when we switch back to the physical ν representation, in which the tunneling resonance at $eE_z(a + nd) = \varepsilon_g$ is merely a point, at which carriers equally occupy the two subbands. The distinction between results obtained in the ν and j representation seems to be important.

Recently, Harrison and Soref[8] claimed that the electric-field induced anticrossing of WS states in a SL offers the possibility of a population inversion and gain. From a technical point of view, their rate equation approach is problematic. It is seen from Eq. (38) that, e.g., the quantities $f_j^j(\mathbf{k}_\perp, \pm 1)$ do not have the meaning of a local carrier occupation and, therefore, cannot enter any rate equation. This issue has to be clarified. We think that the considered field-induced exchange of the subband population cannot be exploited for the design of an injectorless, intrinsic unipolar midinfrared laser.

The field-dependent redistribution of the carrier density in the double-quantum-well SL clearly differs from the behavior observed in SL's with two subbands in each well treated in Ref. 19. In the latter case, resonant tunneling leads to distinct structures in the field dependence of the carrier occupation. In addition, the occupation of the lower subband always dominates so that a population inversion does not occur. This has to be contrasted with the theoretical results

we obtained for double-quantum-well SL's in this section. Here, the subband populations change gradually with increasing electric field and exchange simply their role, when the subbands are aligned. We do not know the physical reason why the carrier redistribution proceeds so differently in double-quantum-well SL's and single-quantum-well SL's with two occupied subbands. This is an open question which deserves further theoretical investigation. Under these circumstances, an experimental determination of the field-dependent subband occupation, e.g., by PL spectroscopy, and a qualitative comparison with the theoretical results is of great interest.

B. Experimental results

Using PL spectroscopy for the investigation of unipolar (electron) systems implies that the hole distribution serves as a probe for the electron distribution as both the electron *and* hole concentrations determine the intensity. Therefore, either a homogeneous hole distribution is necessary or the hole dynamics must be taken into account for a quantitative determination of the electron subband population from the PL spectra. Using weak, ultrashort excitation pulses for time-resolved detection of the PL signal with a time resolution smaller than the relaxation times for the holes, a homogeneous hole population can be achieved immediately after excitation. The electron populations do not depend on time, since the optically excited electrons can be neglected compared to the ones injected through the contacts. For double-quantum-well SL's, the hole populations p_1 and p_2 of the two quantum wells are equal at time $t=0$, if the absorption is equal in both quantum wells. Under these conditions, the ratio $\rho(0)$ of the PL intensities of the two quantum wells immediately after excitation is equal to the ratio F_1/F_2 of the normalized electron populations. The difference in the well widths in the double-quantum-well SL permits us to identify the two electron subbands by the respective PL energies. Furthermore, it has been shown that the temporal behavior of the PL spectra allows us to determine not only the values of the electron population n_1 and n_2 in each quantum well, but also the hole transfer rates through the barriers.[20] In order to exclude effects of the contacts and the finite length of the SL as well as to compare the experimental with the present theoretical results, F_1 and F_2 have been normalized to the total electron occupation $F=F_1+F_2=1$ for each field strength. From this condition and the equation $\rho(0)=F_1/F_2$, the electron populations are determined. Note that $F_1=n_1/(n_1+n_2)$ and $F_2=n_2/(n_1+n_2)$ with n_1 and n_2 determined according to Ref. 20.

In the experiments, an *n-i-n* structure was used, in which a $GaAs/Al_{0.3}Ga_{0.7}As$ SL with 20 periods forms the intrinsic region. Each period consists of a 4-nm thick quantum well, a 14-nm thick barrier, a 5-nm thick well, and a 10-nm thick barrier. The photoexcitation was carried out by 200-fs pulses of a Ti:sapphire laser. The PL transients were detected using a streak camera with a nominal time resolution of 2 ps. The excitation energy was tuned to 1.72 eV, which is below the energy gap of the barrier material, but well above the interband transition energies for both quantum wells so that homogeneous absorption can be assumed, i.e., $p_0=p_1(0)=p_2(0)$. Figure 4 shows the measured, normalized electron populations F_1 and F_2 of the two quantum wells as a function of the applied electrical field. The experimental data agree qualitatively with the theoretical ones except for the field-induced exchange of the subband population due to tunneling between next nearest cells of the SL, as seen in Fig. 3 at field strengths below 10 kV/cm. These features do not appear in the experimental results due to strong scattering effects. There is no structure in the field-dependent carrier density due to a tunneling resonance, but rather a gradual redistribution of carriers from the lower subband to the higher one, until the population relationship is inverted at high electric fields. In this paper, we focused on a qualitative comparison between experimental data and theoretical results. We arrived at the conclusion that the character of the field-induced carrier redistribution in double-quantum-well SL's differs qualitatively from the redistribution between two subbands in SL's with only one quantum well in the unit cell. A quantitative comparison of experimental and theoretical results requires the detailed consideration of additional scattering mechanisms, which goes beyond the scope of this paper.

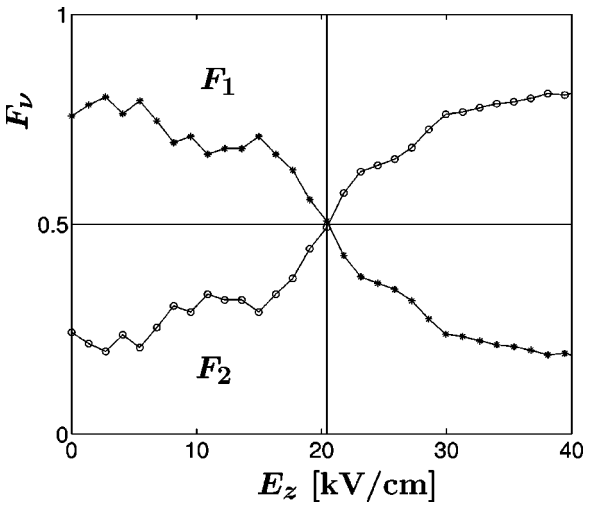

FIG. 4. Measured electron population F_1 and F_2 of the subbands vs applied electric field E_z. The values have been normalized to F_1+F_2 at each field strength.

V. SUMMARY

Carrier redistribution in double-quantum-well SL's has been treated within the density-matrix approach. A simple SL model has been considered, in which each well contains only one level. The interaction-free part of the Hamiltonian has been exactly diagonalized by a canonical transformation. Scattering on polar-optical phonons has been accounted for in the kinetic equations, which have been solved analytically under the assumption that intrasubband scattering is more effective than intersubband scattering.

The carrier redistribution exhibits an interesting field dependence, which is not modified by scattering-induced tunneling. Each time, when levels of the tilted energy scheme

are aligned [$eE_z(a+nd)=\varepsilon_g$, $n=0,1,2,\ldots$], the two subbands are equally populated. At these points, a formal ''population inversion'' occurs, which merely means a relabeling of the upper and lower subband. The same qualitative behavior has also been observed in experiments.

Promising technological applications of double-quantum-well SL's seem to be conceivable only, when at least three subbands are involved in the carrier transport. We hope that our paper provides an orientation for further theoretical work and for the exploration of this exciting area.

ACKNOWLEDGMENTS

We would like to thank R. Hey for the growth of the samples. Support by the Deutsche Forschungsgemeinschaft is gratefully acknowledged by P.K. and V.V.B. in the framework of the German-Russian cooperation and by L.S. and H.T.G. within the Forschergruppe 394.

APPENDIX A: SCATTERING PROBABILITY

The most important quantities in the kinetic equation (39) are the scattering probabilities, which couple different elements of the density matrix to each other. We focus on carrier scattering on polar-optical phonons and replace the coupling term by a constant. In this case, the scattering rate, which consists of scattering-in and scattering-out contributions, is given by

$$
\begin{aligned}
W^{j_1 l_1, j_3 l_3}_{j_2 l_2, j_4 l_4}(\mathbf{k}'_\perp,\mathbf{k}_\perp|t) = {} & \frac{1}{\hbar^2}\sum_{q_z,G} e^{i(l_1-l_2)q_z d}\Pi_{j_1 j_3}(\mathbf{k}'_\perp,\mathbf{k}_\perp|q_z+G,l_1-l_3)\Pi_{j_2 j_4}(\mathbf{k}'_\perp,\mathbf{k}_\perp|q_z+G,l_2-l_4)^* \\
& \times\Bigg\{\int_0^\infty dt e^{-st+i/\hbar[\epsilon_{j_1 l_1}(k'_\perp)-\epsilon_{j_4 l_4}(k_\perp)]t}[(N_0+1)e^{-i\omega_0 t}+N_0 e^{i\omega_0 t}] \\
& +\int_0^\infty dt e^{-st-i/\hbar[\epsilon_{j_2 l_2}(k'_\perp)-\epsilon_{j_3 l_3}(k_\perp)]t}[(N_0+1)e^{i\omega_0 t}+N_0 e^{-i\omega_0 t}]\Bigg\} \\
& -\frac{1}{\hbar^2}\delta_{j_2,j_4}\delta_{l_2,l_4}\delta_{\mathbf{k}'_\perp,\mathbf{k}_\perp}\sum_{j'l'}\sum_{\mathbf{k}''_\perp}\sum_{q_z,G}\Pi_{j' j_3}(\mathbf{k}''_\perp,\mathbf{k}_\perp|q_z+G,l'-l_3)\Pi_{j' j_1}(\mathbf{k}''_\perp,\mathbf{k}_\perp|q_z+G,l'-l_1)^* \\
& \times\int_0^\infty dt e^{-st+i/\hbar[\epsilon_{j'l'}(k''_\perp)-\epsilon_{j_4 l_4}(k_\perp)]t}[(N_0+1)e^{i\omega_0 t}+N_0 e^{-i\omega_0 t}] \\
& -\frac{1}{\hbar^2}\delta_{j_1,j_3}\delta_{l_1,l_3}\delta_{\mathbf{k}'_\perp,\mathbf{k}_\perp}\sum_{j'l'}\sum_{\mathbf{k}''_\perp}\sum_{q_z,G}\Pi_{j' j_2}(\mathbf{k}''_\perp,\mathbf{k}_\perp|q_z+G,l'-l_2)\Pi_{j' j_4}(\mathbf{k}''_\perp,\mathbf{k}_\perp|q_z+G,l'-l_4)^* \\
& \times\int_0^\infty dt e^{-st-i/\hbar[\epsilon_{j'l'}(k''_\perp)-\epsilon_{j_3 l_3}(k_\perp)]t}[(N_0+1)e^{-i\omega_0 t}+N_0 e^{i\omega_0 t}], \qquad \text{(A1)}
\end{aligned}
$$

with the following matrix elements:

$$
\Pi_{j' j}(\mathbf{k}'_\perp,\mathbf{k}_\perp|q_z+G,l)=\sum_{k_z}\sum_{\nu} e^{ilk_z d}\gamma^{\nu}_{\mathbf{k}'_\perp-\mathbf{k}_\perp,q_z+G}\Gamma^{\nu}_{j' j}(\mathbf{k}'_\perp,k_z+q_z|\mathbf{k}_\perp,k_z), \qquad \text{(A2)}
$$

which result from the canonical transformation. N_0 denotes the Bose distribution function and ω_0 the frequency of polar-optical phonons. For simplicity, only bulk phonons are taken into account.

*Email address: kl@pdi-berlin.de

[1] R. F. Kazarinov and R. A. Suris, Fiz. Tekh. Poluprovodn. **5**, 797 (1971) [Sov. Phys. Semicond. **5**, 207 (1971)].
[2] R. F. Kazarinov and R. A. Suris, Fiz. Tekh. Poluprovodn. **6**, 148 (1972) [Sov. Phys. Semicond. **6**, 120 (1972)].
[3] R. F. Kazarinov and R. A. Suris, Fiz. Tekh. Poluprovodn. **7**, 488 (1973) [Sov. Phys. Semicond. **7**, 347 (1973)].
[4] J. Faist, F. Capasso, D. Sivco, A. Hutchinson, and A. Cho, Science **264**, 553 (1994).
[5] V. F. Elesin and Y. V. Kopaev, Zh. Éksp. Teor. Fiz. **108**, 2186 (1995) [Sov. Phys. JETP **81**, 1192 (1995)].
[6] S. Slivken, V. I. Litvinov, and M. Razeghi, J. Appl. Phys. **85**, 665 (1999).
[7] M. Kucharczyk, M. S. Wartak, P. Weetman, and P. Lau, J. Appl. Phys. **86**, 3218 (1999).
[8] P. Harrison and R. A. Soref, IEEE J. Quantum Electron. **37**, 153 (2001).
[9] S. C. Lee and I. Galbraith, Phys. Rev. B **59**, 15 796 (1999).
[10] Q. K. Yang and A. Z. Li, Physica E (Amsterdam) **4**, 239 (1999).
[11] K. Kalna, C. Y. L. Cheung, and K. A. Shore, J. Appl. Phys. **89**,

2001 (2001).
[12] Q. K. Yang and A. Z. Li, J. Phys.: Condens. Matter **12**, 1907 (2000).
[13] S. Tortora, F. Compagnone, A. D. Carlo, and P. Lugli, Physica E (Amsterdam) **7**, 20 (2000).
[14] R. C. Iotti and F. Rossi, Appl. Phys. Lett. **76**, 2265 (2000).
[15] R. C. Iotti and F. Rossi, Appl. Phys. Lett. **78**, 2902 (2001).
[16] V. B. Gorfinkel and S. Luryi, IEEE J. Quantum Electron. **32**, 1995 (1996).
[17] A. Girndt, S. W. Koch, and W. W. Chow, Appl. Phys. A: Mater. Sci. Process. **66**, 1 (1998).
[18] M. C. Wanke, F. Capasso, C. Gmachl, A. Tredicucci, D. L. Sivco, A. L. Hutchinson, S. N. G. Chu, and A. Y. Cho, Appl. Phys. Lett. **78**, 3950 (2001).
[19] P. Kleinert and V. V. Bryksin, Phys. Rev. B **63**, 193303 (2001).
[20] L. Schrottke, R. Hey, and H. T. Grahn, Appl. Phys. Lett. **79**, 629 (2001).
[21] V. V. Bryksin, M. de Dios, and Y. A. Firsov, Fiz. Tverd. Tela **29**, 1141 (1987) [Sov. Phys. Solid State **29**, 651 (1987)].
[22] V. V. Bryksin, Fiz. Tverd. Tela **29**, 2027 (1987) [Sov. Phys. Solid State **29**, 1166 (1987)].
[23] R. C. Iotti and F. Rossi, Phys. Rev. Lett. **87**, 146603 (2001).
[24] V. V. Bryksin and P. Kleinert, J. Phys.: Condens. Matter **9**, 7403 (1997).
[25] P. Kleinert, J. Phys.: Condens. Matter **12**, 8467 (2000).
[26] A. Kristensen, P. E. Lindelof, C. B. Sorensen, and A. Wacker, Semicond. Sci. Technol. **13**, 910 (1998).